Molecular Dynamics Simulations of Human Rhinovirus and an Antiviral Compound

Brent Speelman[¶], Bernard R. Brooks[§], and Carol Beth Post[¶]
[¶]Department of Medicinal Chemistry and Molecular Pharmacology, Purdue University, West Lafayette, Indiana 47907-1333; and
[§]Computational Biophysics Section, National Heart, Lung and Blood Institute, National Institutes of Health, Bethesda, Maryland 20892 USA

ABSTRACT The human rhinovirus 14 (HRV14) protomer, with or without the antiviral compound WIN 52084s, was simulated using molecular dynamics and rotational symmetry boundary conditions to model the effect of the entire icosahedral capsid. The protein asymmetrical unit, comprising four capsid proteins (VP1, VP2, VP3, and VP4) and two calcium ions, was solvated both on the exterior and the interior to fill the inside of the capsid. The stability of the simulations of this large system (~800 residues and 6,650 water molecules) is comparable to more conventional globular protein simulations. The influence of the antiviral compound on compressibility and positional fluctuations is reported. The compressibility, estimated from the density fluctuations in the region of the binding pocket, was found to be greater with WIN 52084s bound than without the drug, substantiating previous computations on reduced viral systems. An increase in compressibility correlates with an entropically more favorable system. In contrast to the increase in density fluctuations and compressibility, the positional fluctuations decreased dramatically for the external loops of VP1 and the N-terminus of VP3 when WIN 52084s is bound. Most of these VP1 and VP3 loops are found near the fivefold axis, a region whose mobility was not considered in reduced systems, but can be observed with this simulation of the full viral protomer. Altered loop flexibility is consistent with changes in proteolytic sensitivity observed experimentally. Moreover, decreased flexibility in these intraprotomeric loops is noteworthy since the externalization of VP4, part of VP1, and RNA during the uncoating process is thought to involve areas near the fivefold axis. Both the decrease in positional fluctuations at the fivefold axis and the increase in compressibility near the WIN pocket are discussed in relationship to the antiviral activity of stabilizing the virus against uncoating.

INTRODUCTION

Human rhinovirus (HRV), a member of the picornavirus family, is the cause of approximately 50% of common colds. The structure of HRV14 (one of more than 100 serotypes of HRV) with and without the antiviral drug, WIN 52084s, has been determined by x-ray crystallography (Rossmann et al., 1985; Smith et al., 1986). The protein coat of the capsid has icosahedral symmetry and consists of four viral proteins: VP1, VP2, VP3, and VP4. These proteins encapsulate approximately 7200 nucleotides of the viral positive-stranded RNA. Drugs in the WIN family are effective inhibitors of viral replication, and one is currently being investigated as a commercial therapeutic agent (Pevear et al., 1999). Therefore, determining the mechanism of inhibition of this class of drugs is important and could lead to further increases in efficacy and to the design of novel antiviral agents.

WIN drugs are commonly effective inhibitors of multiple serotypes of HRV and even other picornaviruses, such as enterovirus and poliovirus (Badger et al., 1988; Chow et al., 1997; Hendry et al., 1999). A conserved eight-stranded β-sandwich in VP1 makes up part of a canyon, or depression in the capsid surface, surrounding the fivefold axis of the capsid. A pocket, which includes part of the interior of this β-sandwich, lies underneath the canyon. The WIN drugs bind into this pocket, displacing water molecules in the case of HRV14 and possibly displacing a long chain molecule, known as pocket factor, that occupies this region in the crystal structure of some picornaviruses (Mosser and Rueckert, 1993; Grant et al., 1994). The binding of these drugs inhibits viral replication (Smith and Baker, 1999) by either inhibiting the attachment of the intercellular adhesion molecule-1 (ICAM-1; Pevear et al., 1989) or stabilizing the capsid and preventing uncoating which is a necessary step in the viral life cycle (Fox et al., 1986; Rombaut et al., 1991; Bibler-Muckelbauer et al., 1994). Earlier investigations using stochastic boundary molecular dynamics of a reduced viral system found that binding of WIN 52084s to HRV14 increases the compressibility of the capsid (empirically related to an entropically favored conformational state), and weakens the long-range correlations in atomic motions (Phelps and Post, 1995, 1999) as a result of the hydrophobic nature of WIN 52084s (Phelps et al., 1998). An empirical correlation between compressibility and the unfolding entropy of globular proteins leads to the suggestion that WIN 52084s stabilizes the protein capsid and prevents uncoating by increasing the configurational entropy of the capsid. This basis for antiviral activity predicted from theory is supported by recent experimental evidence (Tsang et al., 2000).

In the following, we extend earlier molecular dynamics studies (Phelps et al., 2000) that focused on a localized region centered on the WIN 52084s binding pocket, by simulating the time-dependent dynamics of the entire viral

Received for publication 2 June 2000 and in final form 28 September 2000.
Address reprint requests to Carol Beth Post, Department of Medicinal Chemistry and Molecular Pharmacology, Purdue University, West Lafayette, Indiana 47907-1333. Tel.: 765-494-5980; Fax: 765-496-1189; E-mail: cbp@cc.purdue.edu.

0006-3495/01/01/121/09 $2.00

capsid with and without the drug WIN 52084s, using molecular dynamics with rotational symmetry boundary conditions (Cagin et al., 1991; Yoneda et al., 1996). Thus, the effect of an extremely large system (nearly 2×10^6 protein and water atoms) with interpenetrating protein chains can be simulated by taking advantage of the icosahedral symmetry. Additionally, we investigate the influence of the antiviral compound on positional fluctuations of the virus and viral compressibility. WIN 52084s is found to greatly dampen the fluctuations in loops of the capsid near the fivefold axis. This observation is intriguing, given the putative role of this region in uncoating (Fricks and Hogle, 1990; Giranda et al., 1992; Mosser and Rueckert, 1993; Belnap et al., 2000). These effects are also discussed in terms of the susceptibility of the virus to enzymatic cleavage (Lewis et al., 1998).

METHODS

The molecular dynamics calculations for both the free HRV14 and the HRV14·WIN 52084s complex were performed using the CHARMM program (Brooks et al., 1983). The icosahedral, rotational boundary method (Cagin et al., 1991), which effectively reproduces the entire viral capsid, was implemented with the IMAGES facility within CHARMM. The rotational boundary method utilizes rotational symmetry to form a roughly spherical object from identical units, in contrast to the space-filling translational symmetry of periodic boundary methods. Interatomic interactions were calculated using the minimum image convention, with new coordinate positions for primary and image atoms obtained at each step. An update of the image list was made at 20-step intervals. At the center of the icosahedral sphere, primary atoms and image atoms are necessarily separated by a distance shorter than the nonbond cutoff distance. As a result, the interactions between these water molecules are not accurately modeled. Nevertheless, the effect on the dynamics of the virus from this computational inaccuracy is assumed to be insignificant, because the inside radius of the protein shell is 90 Å from the center of the sphere.

Initial velocities were assigned randomly corresponding to 100 K, and the system was heated to 300 K over a time of 30 ps. The system was allowed to equilibrate over a 170-ps period. Velocities were scaled during this period to maintain the temperature near 300 K, with the last scaling at approximately 80 ps. During the subsequent 800-ps analysis period, the temperature remained constant on average without velocity scaling. A force switching function (Steinbach and Brooks, 1994) was used to smoothly truncate electrostatic and van der Waals nonbonded forces at a cutoff of 11.0 Å. The covalent bonds to hydrogen atoms were restrained with the SHAKE algorithm. The equations of motion were integrated using the Verlet leap-frog algorithm and a time step of 1 fs. A nonbonded list update was performed every 20 steps. A spherical quadratic potential was used to restrain exterior water molecules at the outer boundary (Beglov and Roux, 1994).

The coordinates used for the asymmetrical unit were either HRV14 (protein data bank: 4RHV; Rossmann et al., 1985) or HRV14·WIN 52084s (protein data bank: 2RS1; Smith et al., 1986). The CHARMM version 22 all-hydrogen parameter set was used. Implicit hydrogen parameters for WIN 52084s (Lybrand and McCammon, 1988) were modified to reflect the use of explicit hydrogens. Parameters for bond length, bond angle, and dihedral angle terms, as well as nonbonded interactions, were added or modified using chemically similar groups from the CHARMM version 22 all-hydrogen parameter set. The partial charges assigned to WIN 52084s are shown in Table 1.

Electron density at the threefold and fivefold symmetry axes has been interpreted as calcium ions (Zhao et al., 1997). In order to simulate a calcium ion located on a symmetry axis under icosahedral boundary conditions, it was necessary to develop a single-atom model that conforms to the symmetry requirements. Therefore, the calcium ion was subdivided according to its location. A sub-calcium ion was placed on the threefold axis near the carboxylate side chain of Glu 200 of VP3 and on the fivefold axis near the backbone carbonyl oxygen of Asp 141 of VP1 (Zhao et al., 1997). These sub-calcium ions, with a charge of +2/5 on the fivefold axis and + 2/3 on the threefold axis, were offset approximately 0.1 Å from the axis within the asymmetrical unit. An image update was performed to create the two (for the threefold axis) or four (for the fivefold axis) sub-calcium ion image neighbors using the icosahedral, rotational symmetry operations. The primary sub-calcium ion was bonded to all calcium image neighbors. Each image sub-calcium ion was also bonded to its other two (for the threefold) or four (for the fivefold) neighbors. Consequently, these symmetry related sub-calcium ions create an effective pseudo-calcium ion (charge +2) centered directly on the threefold or fivefold axis. These pseudo-calcium ions are therefore constrained, with no lateral diffusion off the symmetry axis; however, they are free to move along the axis

TABLE 1 Atomic partial charges for WIN 52084s

Name	Type	Charge	Name	Type	Charge	Name	Type	Charge
C3	CPH2	0.23	H12	HA	0.10	C5*	CA	−0.12
C4	CPH1	0.16	H21	HAL	0.09	C6*	CA	−0.12
C5	CPH	−0.03	H22	HAL	0.09	H2*	HP	0.12
O1	ON6	−0.29	H31	HAL	0.09	H3*	HP	0.12
N2	NR2	0.41	H32	HAL	0.09	H5*	HP	0.12
C31	CT3	−0.20	H41	HAL	0.09	H6*	HP	0.12
H1	HA	0.10	H42	HAL	0.09	C2′	CN6B	0.11
H2	HA	0.10	H51	HAL	0.09	O1′	ON6	−0.27
H3	HA	0.10	H52	HAL	0.09	N3′	NN5	−0.40
HC4	HR3	0.10	H61	HAL	0.09	C4′	CN6	0.14
C1#	CT2	−0.09	H62	HAL	0.09	C5′	CN6	0.11
C2#	CTL2	−0.15	H71	HAL	0.09	CM1	CT3	−0.23
C3#	CTL2	−0.18	H72	HAL	0.09	HM1	HA	0.09
C4#	CTL2	−0.18	O1*	OH1	−0.40	HM2	HA	0.09
C5#	CTL2	−0.18	C1*	CA	0.11	HM3	HA	0.09
C6#	CTL2	−0.12	C2*	CA	−0.12	H1′	HN6	0.09
C7#	CTL2	0.05	C3*	CA	−0.12	H2′	HN6	0.09
H11	HA	0.10	C4*	CA	0.00	H3′	HN6	0.09

and mimic fluctuations in the plane perpendicular to the axis through bond vibrations between the sub-calcium ions.

In order to solvate the viral capsid, an equilibrated box of TIP3 water molecules was overlaid on the virus in a series of positions so as to fill the asymmetrical unit of the capsid. A water molecule within 2.8 Å of any crystallographic protein atom, calcium ion, WIN 52084s, or other water molecule was deleted. Water molecules were relaxed by steepest descent energy minimization while holding the protein, calcium, and WIN 52084s coordinates fixed. The entire system was then minimized without any restrictions. A second overlay following the same protocol was done to fill voids that could result from energy minimization.

RNA, which does not have icosahedral symmetry and is therefore crystallographically transparent, was not modeled in this simulation. Instead the viral capsid was filled with water molecules, as illustrated in Fig. 1.

Fractional density fluctuations around WIN 52084s were calculated within an 18-Å cube centered at approximately the middle of WIN 52084s. The fractional density was determined using a constant-volume grid with 0.1 Å spacing by calculating the fraction of grid points that resided within the van der Waals radius of a protein, WIN 52084s, or water atom. Fluctuations were determined over a time period of 800 ps with 0.2-ps increments.

The asymmetrical unit of the simulation has 12,432 protein atoms, 19,953 water atoms, and 2 calcium ions (Fig. 1 *c*). WIN 52084s is composed of 54 atoms. Using the symmetry conditions, in effect, the entire viral capsid consisting of approximately 750,000 protein atoms can be modeled.

The simulations were performed using a parallel version of CHARMM 27 running on a Beowulf class supercomputer consisting of a cluster of 100 dual Intel Pentium II computers connected with a gigabit network. Using six processors, 32 ps/day of the HRV14 capsid system were simulated. Additionally, 5 nodes of a 20-node Intel Pentium III cluster, also with gigabit network connections, were used and had a performance of 31 ps/day.

RESULTS

The protomeric unit of HRV14 (Fig. 1 *B*), comprised of four viral proteins, interacts extensively with neighboring protomers. The location of the asymmetrical unit is shown in relation to the entire HRV14 viral capsid in Fig. 1 *A*. The solvated asymmetrical unit, with WIN 52084s represented as space filling atoms, is shown Fig. 1 *C* with the fivefold axis running approximately along the right side of the wedge and the threefold axis along the left side. The calcium ions (magenta spheres) are located near the exterior of the capsid. Molecular dynamics simulations of solvated HRV14, with and without WIN 52084s, were calculated for 1 ns and included effects of neighboring protomers by the use of icosahedral symmetry conditions. In addition to the icosahedral symmetry conditions, water molecules were subjected to a quartic boundary force (Beglov and Roux, 1994) at the exterior of the spherical system (~160 Å radius). Both simulation systems were stable based on con-

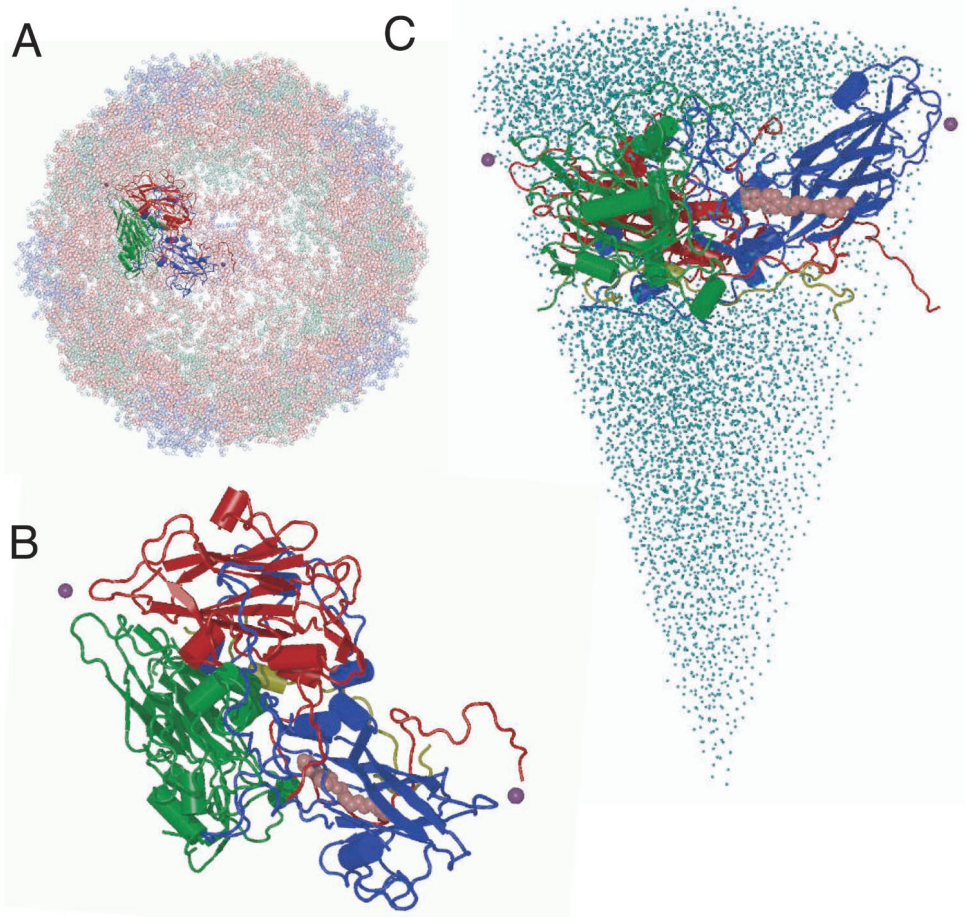

FIGURE 1 (*A*) The protomeric unit of HRV14 (CHARMM energy minimized x-ray structure) comprising VP1 (blue), VP2 (green), VP3 (red), and VP4 (yellow) in relation to the whole HRV14 viral capsid. (*B*) A larger representation of the protomeric unit. (*C*) The solvated system (wedge) with water oxygen atoms represented as cyan spheres and the calcium ions as purple spheres. The protomeric unit is related to *B* by a 90° rotation. These diagrams were produced with VMD (Humphrey et al., 1996) and Raster3D (Merritt and Bacon, 1997).

servation of energy and maintenance of a constant average temperature of 300 K. Furthermore, the capsid, with or without WIN 52084s, remained well solvated for the 1-ns simulation period; the most radially distant protein atoms remained solvated by three layers of water molecules. Thus, the combination of a spherical quadratic boundary potential (Beglov and Roux, 1994) and icosahedral rotational symmetry conditions (Cagin et al., 1991; Yoneda et al., 1996) maintained the initial distribution of solvation waters at the exterior boundary.

The root mean square deviations (RMSD) between simulation coordinate snapshots (taken every 0.2 ps) and the minimized crystallographic coordinates for the backbone atoms of HRV14 with and without WIN 52084s are shown in Fig. 2 *A*. The RMSD of HRV14·WIN 52084s remains relatively constant over the time of the simulation at approximately 1.5 Å, a value typical of globular protein simulations (Post and Dadarlat, 2000). The overall RMSD of the backbone atoms for HRV14 is slightly larger and averages approximately 2.0 Å.

The backbone RMSD values shown in Fig. 2, *B-E*, are for the separate protein chains of the capsid. Both VP2 and VP3 main chain deviations are fairly constant, whereas VP1 and VP4 show larger coordinate differences for either the HRV14 or the HRV14·WIN 52084 system. An increase in the RMSD for VP1 in free HRV14 at approximately 510 ps results primarily from motions of the BC, DE, and GH loops of VP1.

The heavy atom RMSD values for the drug, WIN 52084s, are shown in Fig. 3. The RMSD is ~4 Å at the beginning of the simulation, followed by a steady movement closer to the initial energy-minimized crystallographic position. This magnitude of coordinate deviation is relatively large. Although it is reasonable that larger coordinate deviations

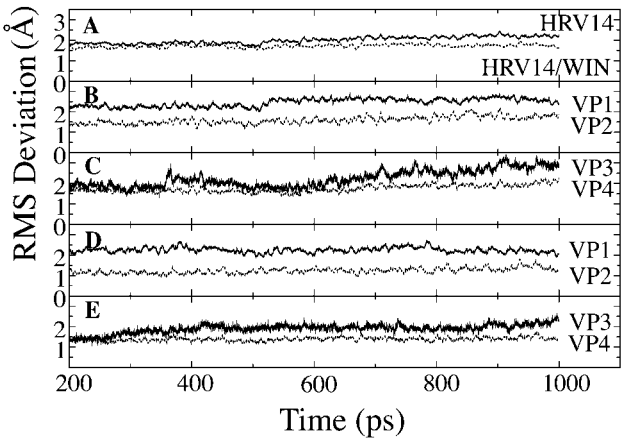

FIGURE 2 The RMS coordinate deviation between the simulation structure and the energy-minimized crystal structure as a function of time for (*A*) the protein backbone atoms of HRV14 and HRV14·WIN 52084s (*dashed line*), (*B*) the backbone atoms of VP1 and VP2 (*dashed line*) for HRV14, (*C*) the backbone atoms of VP3 and VP4 (*dashed*) for HRV14, (*D*) the backbone atoms of VP1 and VP2 (*dashed*) for HRV14·WIN 52084s, and (*E*) the backbone atoms of VP3 and VP4 (*dashed*) for HRV14·WIN 52084s.

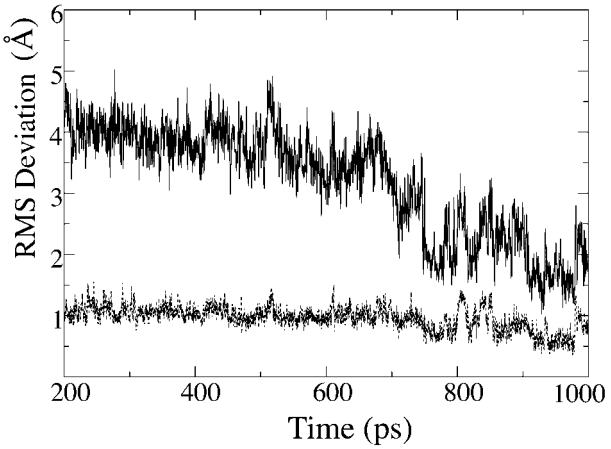

FIGURE 3 The RMS coordinate deviation between the energy-minimized crystal structure as a function of time for the heavy atoms of WIN 52084s after orientation with respect to the minimized crystal structure of the protein (*top*) or orientation with respect to the WIN 52084s atoms (*bottom*).

between simulation and crystallographic structures could occur for simulations initiated with low resolution or unrefined crystallographic coordinates, a previous investigation did not find such a correspondence (Post and Dadarlat, 2000). Thus, additional simulations were calculated. Similar RMSD values for WIN 52084s were observed in three independent trajectories using different initial velocities. In one of the additional simulations, the RMSD of WIN 52084s after 200 ps was 2.7 Å, yet the RMSD for the backbone atoms was 1.8 Å, indicating that the overall structure was not sensitive to the position of the drug. The RMSD values calculated for WIN 52084s after a best fit superposition to the initial energy-minimized WIN 52084s coordinates (Fig. 3) are 1 to 1.5 Å, considerably less than the 2 to 4 Å values obtained without superposition, and indicate that the general shape of the drug molecule does not vary significantly. Together, these factors suggest that the observed mobility of the drug in the pocket is a physical characteristic of the drug molecule rather than a result of inaccuracy in the initial crystallographic coordinates or assigned velocities. This feature is considered further in Discussion.

The heavy atom RMSD values for the calcium ions at the threefold axis, shown in Fig. 4, *A* and *B*, are less than those of the calcium ion at the fivefold axis (Fig. 4, *C* and *D*). The calcium at the fivefold axis moved to a position toward the exterior of the capsid to become partially solvated and with less contact with the five symmetry-related carbonyl oxygens of Asn 141 of VP1.

Density fluctuations

The isothermal compressibility was estimated from the simulations to assess the effect of WIN 52084s and probe the basis of antiviral activity. Density fluctuations were deter-

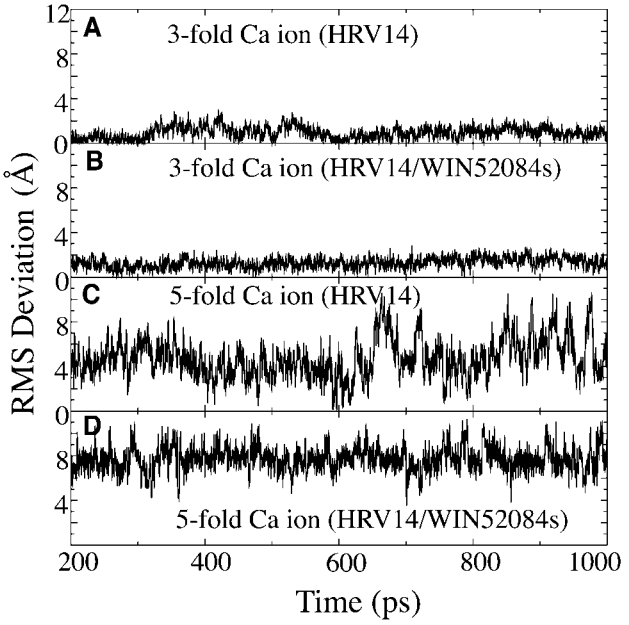

FIGURE 4 The RMS coordinate deviation between the energy-minimized structure as a function of time for (*A*) the threefold calcium ion of HRV14, (*B*) the threefold calcium ion of HRV14·WIN 52084s, (*C*) the fivefold calcium ion of HRV14, and (*D*) the fivefold calcium ion of HRV14·WIN 52084s.

mined for an 18-Å cube around the drug, analogous to calculations from previous stochastic boundary molecular dynamics simulation (Phelps and Post, 1995). The isothermal compressibility was calculated using the following equation:

$$\beta_T = \frac{\langle(\rho - \bar{\rho})^2\rangle V}{\bar{\rho}^2 kT}$$

where β_T is the isothermal compressibility, ρ is the fractional particle density, V is the volume of the cube, and kT has its usual meaning. β_T for HRV14 was 14.8×10^6 bar^{-1} and increases for HRV14·WIN52084 to 19.4×10^6 bar^{-1}. This increase is the same trend found in previously (Table 2) and is consistent with an increase in the entropy in the presence of WIN 52084s. The more favorable configurational entropy of HRV14·WIN52084 would inhibit uncoating.

Positional fluctuations

The RMS fluctuations of the backbone atoms averaged over the simulation for each protein residue are shown in Fig. 5, *A-F*. Estimates from crystallographic temperature factors (B values) for free HRV14 are also shown and were obtained using the equation:

$$\langle \Delta R^2 \rangle^{1/2} = (3B/8\pi^2)^{1/2}.$$

The qualitative character of the temperature factors is reproduced well by the simulation for the major proteins VP1, VP2, and VP3. In particular, the fluctuations of VP1 loops connecting the strands of the β-sandwich (residues 89–99, 136–145, and 154–173) near the fivefold axis of the capsid correlates with the crystallographic data as shown in Fig. 5 *A*. A comparison for HRV14·WIN52084 is not possible, because the crystallographic B values are not available.

The fluctuations of the backbone atoms of the capsid with WIN 52084s bound were compared to the fluctuations of the capsid without the drug bound. Large changes are seen in the N-terminal coil region of VP1, the BC loop (residues 89–91), DE loop (residues 136–140), EF loop (residues 156–169), and GH loop (residues 209–210), which have greatly dampened fluctuations with the drug bound. These loops are shown from two views in Fig. 6, *A* and *B*. The residues with the color blue represent regions with the greatest decrease in fluctuations when WIN 52084s is bound. Additionally, the N-terminus of VP3 had much smaller fluctuations with WIN 52084s bound.

TABLE 2 Calculated isothermal compressibilities

Simulation	WIN 52084s	β_T
Icosahedral* boundary	no	14.8×10^6 bar^{-1}
Icosahedral* boundary	yes	19.4×10^6 bar^{-1}
Stochastic† boundary	no	8.9×10^6 bar^{-1}
Stochastic† boundary	yes	11.8×10^6 bar^{-1}

*This work.
†Phelps and Post, 1995.

DISCUSSION

Until the recent advances in computational power, simulating the protein coat of an entire icosahedral virus would have been futile. Parallel computing and rotational symmetry methods have made feasible the simulation of an ~800-residue, fully solvated macromolecular system. The rotational boundary method, which uses icosahedral symmetry to include the neighboring protomers in the environment of the viral capsid, is essential, since image protein chains penetrate the asymmetrical unit to form substantial inter-protomeric contacts.

Although the viral capsid is a complex system, the simulations display good stability. Previous simulations of the virus protomer using either an implicit water model for solvation or a less extensive wedge of water molecules were run no longer than 60 ps (Cagin et al., 1991; Yoneda et al., 1996). For this study of the protomer with WIN 52084s bound, a system consisting of four protein chains, one multiring drug molecule, calcium ions, and approximately 6600 water molecules had good stability with a backbone RMS deviation from the minimized structure of only 1.5 Å after 1 ns of dynamics. Using stochastic boundary molecular dynamics, a simulation of a 22 Å spherical region of HRV14 centered in the pocket which contains WIN 52084s had an average RMS deviation of 1.9 Å after 800 ps. These RMSD values are similar to globular protein simulations (Post and Dadarlat, 2000) and demonstrate the utility of the rotational symmetry

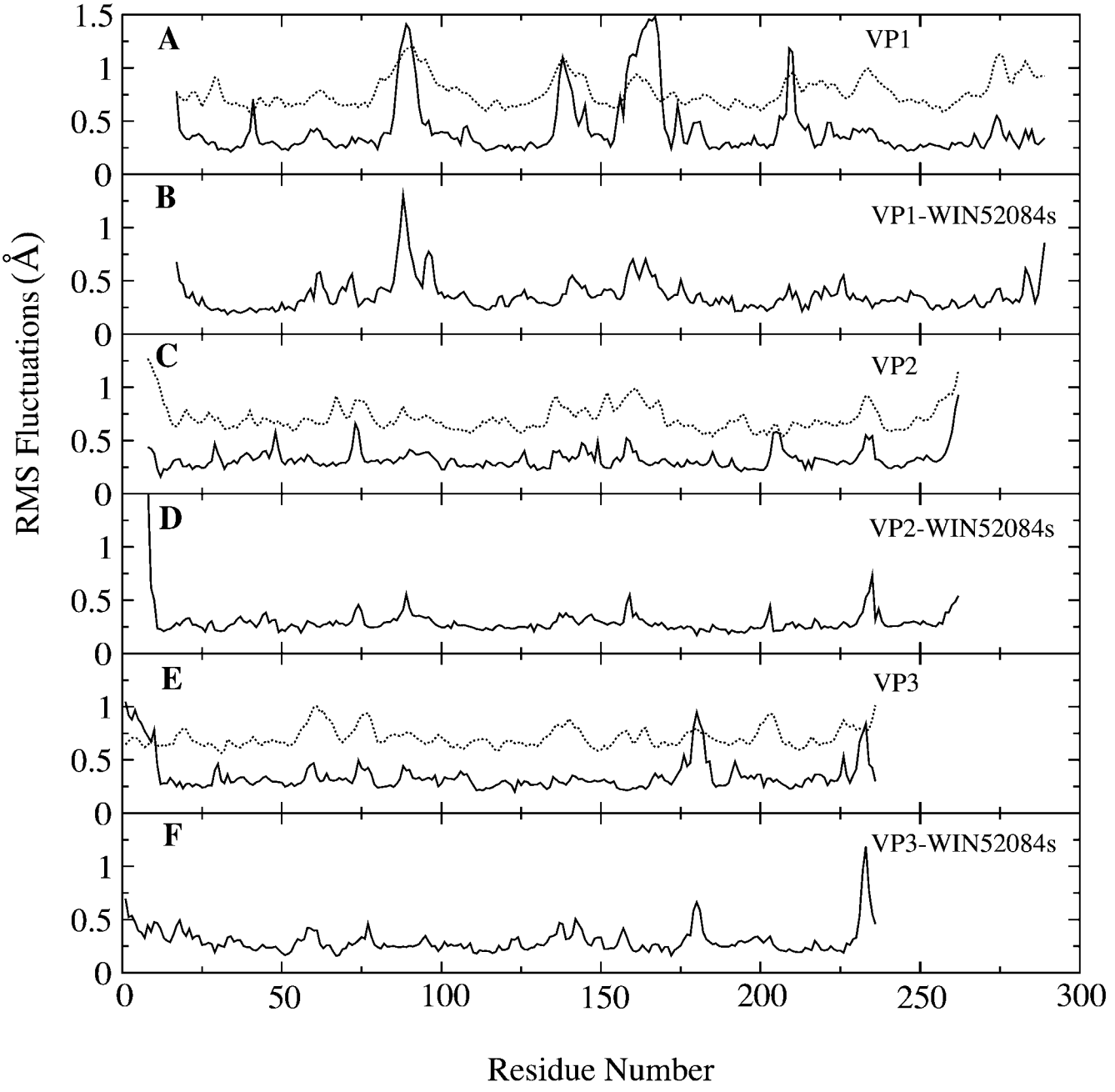

FIGURE 5 The RMS fluctuations of the backbone atoms calculated from the molecular dynamics trajectory (*solid lines*), and the scaled temperature or B factors from crystal structure (*dashed line*) as a function of residue number for (*A*) VP1 of HRV14, (*B*) VP1 of HRV14·WIN 52084s, (*C*) VP2 of HRV14, (*D*) VP2 of HRV14·WIN 52084s, (*E*) VP3 of HRV14, and (*F*) VP3 of HRV14·WIN 52084s. The RMS fluctuations were calculated over a time period from 200 to 1000 ps. The decreased fluctuations in VP1 of HRV14·WIN 52084s occur in the N-terminal coil region of VP1, the BC loop (residues 89–91), DE loop (residues 136–140), EF loop (residues 156–169), and GH loop (residues 209–210).

method and the suitability of the CHARMM force field for simulating solvated icosahedral viruses.

Effect of WIN 52084s on viral conformational mobility

The N-terminus of VP3, which appears as an isolated red coil on the right side of Fig. 1, *B* and *C*, is crystallographically defined in its entirety and forms a β-barrel-like structure with the four other symmetry related N-termini of VP3 around the fivefold axis of the capsid. This structure stabilizes the pentamer by interactions about the fivefold vertex. The N-terminus of VP3 has much larger fluctuations in the absence of WIN 52084s than with WIN 52084s bound. Larger fluctuations in the absence of WIN 52084s are also seen for the loops at the extremities of the capsid, and near

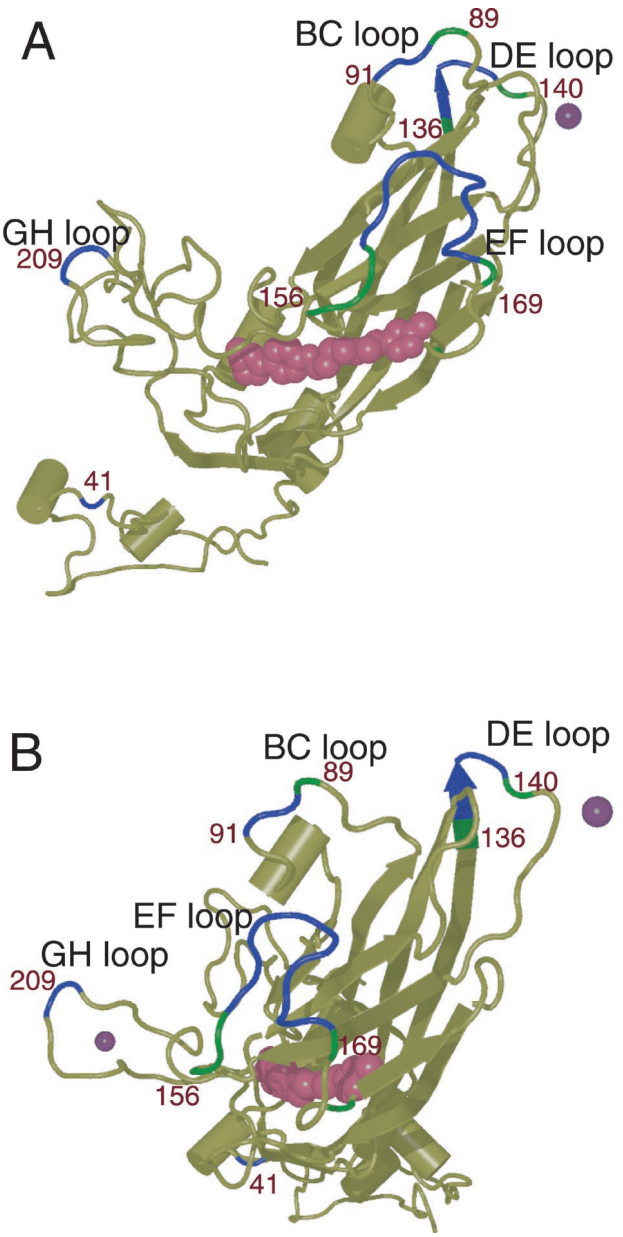

FIGURE 6 VP1 of HRV14 capsid with WIN 52084s (*magenta*) and calcium ions (*purple*) with color coded areas showing regions with diminished fluctuations when WIN 52084s is bound. Green areas represent a decrease of fluctuations of 0.3 to 0.49 Å and blue areas represent a decrease of greater than 0.5. VP1 is shown in two orientations: (*A*) an orientation similar to Fig. 1 *C*, and (*B*) rotated approximately 70° about a vertical axis.

the fivefold axis (Fig. 6). How WIN 52084s affects so profoundly the magnitude of the fluctuations of relatively isolated loop structures distant from the binding pocket is unclear, but intriguing, given that VP4 and RNA are hypothesized to exit the viral capsid by mechanisms involving protein contacts at or near the fivefold axes (Mosser and Rueckert, 1993; Giranda et al., 1992; Belnap et al., 2000). One model for uncoating suggests externalization of VP4 and RNA at the fivefold axes (Mosser and Rueckert, 1993; Giranda et al., 1992) which would require a certain conformational flexibility in this region. The large, picosecond-timescale fluctuations of these intrapentameric loops suggests a substantial conformational flexibility for HRV14 that could facilitate structural transitions required for uncoating. The diminution in fluctuations, seen here in the presence of WIN 52084s, could inhibit such externalization and is consistent with a more rigid structure described by an earlier computational study (Vaidehi and Goddard, 1997). Alternatively, low-resolution structural studies of the 135S particle of poliovirus indicate that the N-terminus of VP1 and VP4 are released by disrupting VP1-VP1 interactions near the base of the canyon and close to the EF loop by a pivot-like motion at the fivefold axis (Belnap et al., 2000). This model would imply flexibility in the BC, DE, EF, and GH loops, all regions for which the fluctuations are altered in the presence of WIN 52084s. Thus, the antiviral activity of inhibiting an uncoating process that involves disruption of VP1-VP1 interactions can also be understood from the reduced mobility observed in the simulations.

A greater configurational entropy of poliovirus in the presence of drug molecules has been measured experimentally (Tsang et al., 2000). Indeed, an increase in entropy was predicted based on compressibility calculations from simulations of a reduced system (Phelps and Post, 1995). These previous results are now substantiated with simulations of an improved model of the full protomer reported here. The loss of local entropy associated with the reduced fluctuations in the VP1 loops would partially compensate for an increase in configurational entropy with WIN 52084s bound (indicated from the increased compressibility measured in the region of the binding pocket). Such compensation in entropy has been noted in earlier studies. Structural studies of adenylate kinase found that the binding of a competitive inhibitor leads to an increase in protein chain mobility far from the active site, whereas the region of the protein involved in binding becomes less mobile (Müller et al., 1996). Such compensation effects distant from a binding site have also been noted in molecular dynamics studies (Post et al., 1986; Harte et al., 1992). In these earlier reports, specific polar interactions between an enzyme and a ligand rigidify a previously mobile active site of the unligated enzyme. As such, the compensatory changes in mobility are opposite in direction to those of WIN 52084s; association of WIN 52084s, a hydrophobic compound with nondirectional apolar interactions, leads to higher mobility in the binding site countered by less mobile loops of VP1 distant from the binding site.

The smaller fluctuations when WIN52084 is bound are also noteworthy in view of the lack of cleavage by trypsin of the capsid in limited proteolysis/mass spectrometry studies (Lewis et al., 1998). These investigators found that HRV14 is cleaved at a variety of sites during limited proteolysis, but the presence of a WIN compound fully protects HRV14 against all detectable cleavage. Large amplitude fluctuations are necessary for proteolysis. Thus, the confor-

mational restrictions in the presence of the drug may relate to the observed protection against proteolytic enzymes. For example, one cleavage site is reported to be in the BC loop of VP1, and the binding of the antiviral drug results in a lowering in the fluctuations at the C-terminal end of the loop (residues 95–98). These are also residues found to be important in binding the receptor, ICAM-1, and antibodies (Smith and Mosser, 1997; Olson et al., 1993).

From these results on limited proteolysis, Lewis and coworkers (1998) proposed that HRV14 exists in two states, one represented by the known crystallographic structure and one with the N-termini of VP1 and VP4 externalized and accessible to proteolytic cleavage. The transition from one state to the other is called "breathing" (Li et al., 1994) and there was postulated to be a small energy barrier to the transformation. In poliovirus, it appears that breathing occurs at 37°C but not at 25°C, based on the accessibility of antibodies to residues normally on the interior of the capsid (Li et al., 1994). The proposal from the simulations of entropically based stabilization in the presence of the drug would be consistent with this two-state breathing model, since the higher configurational entropy of the capsid when the drug is bound favors the state of the known crystallographic structure over the state with the interior residues externalized. Investigating the dynamics by simulations and computation will help elucidate the physiological motions of the capsid and the beginnings of the uncoating process.

The position of WIN 52084s was found to deviate more than the viral protein coordinates from the initial values. It should be noted in this regard that the ligands in the viral pocket are found crystallographically to have disordered electron density and corresponding high B values. Similarly, a hydrophobic ligand binds in a buried pocket between two β-sheets in fatty-acid binding protein and has high B values (Eads et al., 1993; Young et al., 1994). The relatively high mobility of these hydrophobic ligands, as indicated in Table 3 by the ratio of the B value averaged over the atoms of the ligand to that of the protein atoms, is consistent with the dynamic behavior of WIN observed in the simulations. The nondirectional nature of van der Waals forces that associate WIN 52084s to the pocket region of the drug would be expected to confer greater flexibility for drug movement than specific polar or charged interactions. Indeed, it was found that a suspected hydrogen bond between the nitrogen of the oxazoline ring and the amide hydrogen of Asn 219 of VP1 was not important for drug efficacy (Hadfield et al., 1995).

TABLE 3 Temperature factor (B value) ratios for poliovirus and fatty acid binding protein

Ligands	Avg ligand B value/ Avg. protein B value	Protein Data Bank entry
Poliovirus drugs	1.5	1PIV, 1PO1, 1PO2, 1VBD
Poliovirus pocket factor (sphingosine)	1.9	1PVC, 1PLV, 1ASJ, 1POV
Fatty acid binding protein ligands	1.8	1HMS, 1ICM

Calcium ion dynamics

The large fluctuations of the fivefold calcium suggest that coordination by the symmetry-related backbone carbonyls of ASN 141 of VP1 is not highly favorable. The ion on the fivefold axis appears to prefer solvation by water to coordination by the backbone of VP1. On the other hand, the calcium at the threefold axis has much smaller fluctuations and appears to be tightly bound to the much more electron-rich ASP 200 (of VP3) side chain carboxyl groups. It would appear that the additional flexibility of the side chain would allow efficient coordination of the calcium ion on the threefold axis, whereas at the fivefold axis, the coordinated movements of the backbone would allow less freedom of the carbonyl to optimize ion coordination. Indeed, HRV14 crystals soaked in EGTA showed no conformational changes despite the loss of the putative calcium ion on the fivefold axis (Zhao et al., 1997). Therefore, the calcium ion at the fivefold axis is probably not a significant stabilizing factor for the protein capsid. The five symmetry-related backbone carbonyl oxygens could indeed provide a binding site for a cation (Zhao et al., 1997; Kalko et al., 1992); however, the cation is not necessary to maintain this structure at the fivefold axis.

Interestingly, in poliovirus, electron density on the fivefold axis was attributed to chloride (Hogle et al., 1985). Additionally, the density of the putative calcium ion in HRV14 and group B coxsackievirus (Zhao et al., 1997; Muckelbauer et al., 1995) was found to be less at the fivefold than at the threefold axis. Thus, cation binding at the threefold axis appears to be more favorable than binding at the fivefold axis and may not be necessary for interprotomer stability.

This work was supported by National Institutes of Health grant AI39639 to C. B. P. and a Research Career Development Award K04-GM00661. The Structural Biology group at Purdue received support from the Lucille P. Markey Foundation and the Purdue University Academic Reinvestment Program. The computations were done on the LoBoS, a Beowulf cluster of the Computational Biophysics Section at National Institutes of Health and an Intel cluster provided by Intel Corporation through the Technology for Education 2000 Project.

REFERENCES

Badger, J., I. Minor, M. J. Kremer, M. A. Oliveira, T. J. Smith, J. P. Griffith, D. M. A. Guerin, S. Krishnaswamy, M. Luo, M. G. Rossmann, M. A. McKinlay, G. D. Diana, F. J. Dutko, M. Fancher, R. R. Rueckert, and B. A. Heinz. 1988. Structural analysis of a series of antiviral agents complexed with human rhinovirus 14. *Proc. Natl. Acad. Sci. USA.* 85:3304–3308.

Beglov, D., and B. Roux. 1994. Finite representation of an infinite bulk system: solvent boundary potential for computer simulations. *J. Phys. Chem.* 100:9050–9063.

Belnap, D. M., D. J. Filman, B. L. Trus, N. Cheng, F. P., Booy, J. F. Conway, S. Curry, C. N. Hiremath, S. K. Tsang, A. C. Steven, and J. M. Hogle. 2000. Molecular tectonic model of virus structural transitions: the putative cell entry states of poliovirus. *J. Virol.* 74:1342–1354.

Bibler-Muckelbauer, J. K., M. J. Kremer, M. G. Rossmann, G. D. Diana, F. J. Dutko, D. C. Pevear, and M. A. McKinlay. 1994. Human rhinovirus 14 complexed with fragments of active antiviral compounds. *Virology.* 202:360–369.

Brooks, B. R., R. E. Bruccoleri, B. D. Olafson, D. J. States, S. Swaminathan, and M. Karplus. 1983. CHARMM: a program for macromolecular energy, minimization, and dynamics calculations. *J. Comp. Chem.* 4:187–217.

Cagin, T., M. Holder, and B. M. Pettitt. 1991. A method for modeling icosahedral virions: rotational symmetry boundary conditions. *J. Comp. Chem.* 12:627–634.

Chow, M., R. Basavappa, and J. M. Hogle. 1997. The role of conformational transitions in poliovirus pathogenesis. *In* Structural Biology of Viruses. W. Chiu, R. M. Burnett, and R. L. Garcea, editors. Oxford University Press, New York. 157–186.

Eads, J. C., J. C. Sacchettini, A. Kromminga, and J. I. Gordon. 1993. Escherichia coli-derived rat intestinal fatty acid binding protein with bound myristate at 1.5 Å resolution and I-FABP Arg106→Gln with bound oleate at 1.74 Å resolution. *J. Biol. Chem.* 268:26375–26385.

Fox, M. P., M. J. Otto, and M. A. McKinlay. 1986. The prevention of rhinovirus and poliovirus uncoating by WIN 51711: a new antiviral drug. *Antimicrob. Agents Chemother.* 30:110–116.

Fricks, C. E., and J. M. Hogle. 1990. Cell-induced conformational change in poliovirus: externalization of the amino terminus of VP1 is responsible for liposome binding. *J. Virol.* 64:1934–1945.

Grant, R. A., C. N. Hiremath, D. J. Filman, R. Syed, K. Andries, and J. M. Hogle. 1994. Structures of poliovirus complexes with antiviral drugs: implications for viral stability and drug design. *Curr. Biol.* 4:784–797.

Hadfield, A. T., M. A. Oliveira, K. H. Kim, I. Minor, M. J. Kremer, B. A. Heinz, D. Shepard, D. C. Pevear, R. R. Rueckert, and M. G. Rossmann. 1995. Structural studies on human rhinovirus 14 drug-resistant compensation mutants. *J. Mol. Biol.* 253:61–73.

Harte, W. E., Swaminathan, S., and D. L. Beveridge. 1992. Molecular-dynamics of HIV-1 protease. *Proteins Struct. Funct. Genet.* 13:175–194.

Hendry, E., H. Hatanaka, E. Fry, M. Smyth, J. Tate, G. Stanway, J. Santti, M. Maaronen, T. Hyypia, and D. Stuart. 1999. The crystal structure of coxsackievirus A9: new insights into the uncoating mechanisms of enteroviruses. *Structure.* 7:1527–1538.

Hogle, J. M., M. Chow, and D. J. Filman. 1985. The three dimensional structure of poliovirus at 2.9A resolution. *Science.* 229:1358–1365.

Humphrey, W., A. Dalke, and K. Schulten. 1996. VMD: visual molecular dynamics. *J. Mol. Graphics.* 14:33–38.

Kalko, S. G., R. E. Cachau, and S. M. Aberlardo. 1992. Ion channels in icosahedral virus: a comparative analysis of the structures and binding sites at their fivefold axes. *Biophys. J.* 63:1133–1145.

Lewis, K. J., B. Bothner, T. J. Smith, and G. Siuzdak. 1998. Antiviral agent blocks breathing of the common cold virus. *Proc. Natl. Acad. Sci. USA.* 95:6774–6778.

Li, Q., Yafal, A. G., Lee, Y. M., Hogle, J., and M. Chow. 1994. Poliovirus neutralization by antibodies to internal epitopes of VP4 and VP1 results form reversible exposure of these sequences at physiological temperature. *J. Virol.* 68:3965–3970.

Lybrand, T. P., and J. A. McCammon. 1988. Computer simulation study of the binding of an antiviral agent to a sensitive and resistant human rhinovirus. *J. Comput. Aided Mol. Design.* 2:259–266.

Merritt, E. A., and D. J. Bacon. 1997. Raster3D: photorealistic molecular graphics. *Methods Enzymol.* 277:505–524.

Mosser, A. G., and R. R. Rueckert. 1993. WIN 51711-dependent mutants of poliovirus type 3: evidence that virions decay after release from cells unless drug is present. *J. Virol.* 67:1246–1254.

Muckelbauer, J. K., M. Kremer, I. Minor, G. Diana, F. J. Dutko, J. Groarke, D. C. Pevear, and M. G. Rossmann. 1995. The structure of coxsackievirus B3 at 3.5 Å resolution. *Structure.* 3:653–667.

Müller, C. W., G. L. Schlauderer, J. Reinstein, and G. E. Schulz. 1996. Adenylate kinase motions during catalysis: an energetic counterweight balancing substrate binding. *Structure.* 4:147–156.

Olson, N. H., P. R. Kolatkar, M. A. Oliveira, R. H. Cheng, J. M. Greve, A. McClelland, T. S. Baker, and M. G. Rossmann. 1993. Structure of a human rhinovirus complexed with its receptor molecule. *Proc. Natl. Acad. Sci. USA.* 90:507–511.

Pevear, D. C., M. J. Fancher, P. J. Felock, M. G. Rossmann, M. S. Miller, G. Diana, A. M. Treasurywala, M. A. McKinlay, and F. J. Dutko. 1989. Conformational change in the floor of the human rhinovirus canyon blocks absorption to HeLa cell receptors. *J. Virol.* 63:2002–2007.

Pevear, D. C., T. M. Tull, M. E. Seipel, and J. M. Groarke. 1999. Activity of pleconaril against enteroviruses. *Antimicrob. Agents Chemother.* 43: 2109–2115.

Phelps, D. K., and C. B. Post. 1995. A novel basis for capsid stabilization by antiviral compounds. *J. Mol. Biol.* 254:544–551.

Phelps, D. K., P. J. Rossky, and C. B. Post. 1998. Influence of an antiviral compound on the temperature dependence of viral protein flexibility and packing: a molecular dynamics study. *J. Mol. Biol.* 276:331–337.

Phelps, D. K., and C. B. Post. 1999. Molecular dynamics investigation of the effect of an antiviral compound on human rhinovirus. *Protein Sci.* 8:2281–2289.

Phelps, D. K., B. Speelman, and C. B. Post. 2000. Theoretical studies of viral capsid proteins. *Curr. Opin. Struct. Biol.* 10:170–173.

Post, C. B., B. R. Brooks, M. Karplus, C. M. Dobson, P. J. Artymiuk, J. C. Cheetham, and D. C. Phillips. 1986. Molecular dynamics simulations of native and substrate-bound lysozyme. *J. Mol. Biol.* 190:455–479.

Post, C. B., and V. M. Dadarlat. 2000. Molecular dynamics simulations of biological macromolecules. *In* International Tables for Macromolecular Crystallography. M.G. Rossmann and E. Arnold, editors. Kluwer Academic, London. In press.

Rombaut, B., K. Andries, and A. Boeye. 1991. A comparison of WIN51711. and R78206 as stabilizers of poliovirus virions and procapsids. *J. Gen. Virol.* 72:2153–2157.

Rossmann, M. G., E. Arnold, J. W. Erickson, E. A. Frankenberger, J. P. Griffith, H. J. Hecht, J. E. Johnson, G. Kamer, M. Luo, A. G. Mosser, R. R. Rueckert, B. Sherry, and G. Vriend. 1985. Structure of a human cold virus and functional relationship to other picornaviruses. *Nature.* 317:145–153.

Smith, T. J., and Baker, T. 1999. Picornaviruses: epitopes, canyons, and pockets. *Adv. Virus Res.* 52:1–23.

Smith, T. J., M. J. Kremer, M. Luo, G. Vriend, E. Arnold, G. Kamer, M. G. Rossmann, M. A. McKinlay, G. D. Diana, and M. J. Otto. 1986. The site of attachment of human rhinovirus 14 for antiviral agents that inhibit uncoating. *Science.* 233:1286–1293.

Smith, T. J., and A. G. Mosser. 1997. Antibody-mediated neutralization of picornaviruses. *In* Structural Biology of Viruses. W. Chiu, R. M. Burnett, and R. L. Garcea, editors. Oxford University Press, New York. 134–156.

Steinbach, P. J., and B. R. Brooks. 1994. New spherical-cutoff methods for long-range forces in macromolecular simulation. *J. Comp. Chem.* 15: 667–683.

Tsang, S. K., P. Danthi, M. Chow, and J. M. Hogle. 2000. Stabilization of poliovirus by capsid-binding antiviral drugs is due to entropic effects. *J. Mol. Biol.* 296:335–340.

Vaidehi, N., and W. A. Goddard, III. 1997. The pentamer channel stiffening model for drug action on human rhinovirus HRV-1A. *Proc. Natl. Acad. Sci. USA.* 94:2466.

Yoneda, S., M. Kitazawa, and H. Umeyama. 1996. Molecular dynamics simulation of a rhinovirus capsid under rotational symmetry boundary conditions. *J. Comp. Chem.* 17:191–203.

Young, A. C., G. Scapin, A. Kromminga, S. B. Patel, J. H. Veerkamp, and J. C. Sacchettini. 1994. Structural studies on human muscle fatty acid binding protein at 1.4 Å resolution: binding interactions with three C18 fatty acids. *Structure.* 2:523–534.

Zhao, R., A. T. Hadfield, M. J. Kremer, and M. G. Rossmann. 1997. Cations in human rhinovirus. *Virology.* 227:13–23.